An Investigation into the Dissipative Stochastic Mechanics Based Neuron Model under Time Varying Input Currents

Amin Almassian

Submitted to the
Institute of Graduate Studies and Research
in partial fulfillment of the requirements for the Degree of

Master of Science
in
Computer Engineering

Eastern Mediterranean University
January 2010
Famagusta, North Cyprus

Approval of the Institute of Graduate Studies and Research

Prof. Dr. Elvan Yılmaz
Director (a)

I certify that this thesis satisfies the requirements as a thesis for the degree of Master of Science in Computer Engineering.

Assoc. Prof. Dr. Muhammed Salamah
Chair, Department of Computer Engineering

We certify that we have read this thesis and that in our opinion it is fully adequate in scope and quality as a thesis for the degree of Master of Science in Computer Engineering.

Prof. Dr. Marifi Güler
Supervisor

Examining Committee

1. Prof. Dr. Marifi Güler
2. Assoc. Prof. Dr. Işık Aybay
3. Asst. Prof. Dr. Adnan Acan

ABSTRACT

Led by the presence of a multiple number of gates in an ion channel, it was recently predicted that the equations of activity for the neuronal dynamics acquire some renormalization terms which play a significant role in the dynamics for smaller membrane sizes (Güler 2006, 2007, 2008). In this Thesis, we examine the resultant computational neuron model, from the above approach, in the case of time varying input currents. In particular, we focus on what role the renormalization terms might be playing in the signal-to-noise ratio values. Our investigation reveals that the presence of renormalization terms somehow enhances the signal-to-noise ratio.

Keywords: Ion Channel Noise, Stochastic Ion Channels, Neuronal Dynamic, Signal-to-Noise Ratio, Stochastic Resonance, Rose-Hindmarsh Model.

ÖZ

Son yıllarda, bir iyon kanalında birden fazla geçit bulunmasından dolayı, nöronal dinamik denklemlerinin ekstra olarak bazı renormalizasyon terimleri içermesi gerekliliği öne sürülmüştür (Güler 2006, 2007, 2008). Ayrıca, bu renormalizasyon terimlerinin küçük boyutlu zarların dinamiği üzerinde önemli bir etkisi olabileceği gösterilmiştir. Bu tezde, yukarıda öne sürülen sinir hücresi modeli zaman değişmeli girdi akımları altında incelenmiştir. Renormalizasyon terimlerinin sinyal-gürültü oran değerleri üzerindeki olası etkileri özellikle çalışılmıştır. Bu çalışma, renormalizasyon terimlerinin sinyal-gürültü oranını arttırdığını göstermiştir.

Anahtar Kelimeler: Iyon Kanalı Gürültüsü, Stokhastik Iyon Kanalları, Nöronal Dinamik, Sinyal-Gürültü Oranı, Stokhastik Resonans, Rose-Hindmarsh Modeli.

DEDICATION

To my dear wife Fatemeh and my beloved parents

ACKNOWLEDGMENTS

I would like to acknowledge with gratitude the supervision of Prof. Dr. Marifi Güler as the research would not have been possible without his knowledge, guidance and effort.

My sincerest gratitude goes to my dear wife and beloved mother and father for their invaluable support, effort and patience who I owe my life and success to them.

TABLE OF CONTENTS

LIST OF FIGURES

Chapter 1

INTRODUCTION

1.1 Introduction

Neurons display electrical activity which is known to be stochastic in nature (Faisal 2008). The primary source of stochasticity in vivo is the external noise from the synapses. However, the intrinsic noise, attributed to the probabilistic character of the gating of an ion channel, can also have significant implications on the dynamic behavior of neurons; as shown both by experimental studies (Sakmann and Neher 1995; Bezrukov and Vodyanoy 1995; Diba et al. 2004; Jacobson et al. 2005; Kole et al. 2006) and by theoretical investigations or numerical simulations (Fox and Lu 1994; Chow and White 1996; Jung and Shuai 2001; Schmid et al. 2001; Rubinstein 1995; Schneidman et al. 1998).

Neuronal dynamics under the influence of channel fluctuations is normally modeled using stochastic differential equations obtained by introducing some white noise terms of vanishing means into the underlying deterministic equations (Fox and Lu 1994). However, the so-called dissipative stochastic mechanics based neuron model (or shortly, "the DSM neuron") was put forward by Güler (2006, 2007), is an exception to this. The DSM model accommodates some functional forms called the renormalization terms, in addition to some white noise terms of vanishing, in the equations of activity. The DSM model has been investigated in detail numerically for

its dynamics for time-independent input currents (Güler 2008); it was found that the renormalization corrections augment the behavioral transitions from quiescence to spiking and from tonic firing to bursting. It was also found that the presence of renormalization corrections can lead to faster temporal synchronization of the respective discharges of electrically coupled two neuronal units (Jibril and Güler 2009). In the present treatise, we examine the DSM model in the case of time varying input currents; in particular, we focus on what role the renormalization terms might be playing in the signal-to-noise ratio values.

1.2 Scope and Organization

In this thesis my attempt is to adhere to the top to bottom approach and to cover essential concepts before dealing with the experiment done and corresponding results. In this sense, after an introduction in chapter 1, a distilled explanation about neuron morphology and the characteristics of neuron known to participate in information processing is presented in chapter 2. In chapter 3, a theme of predominant theories of neuron models is presented and it is followed by explanation of dissipative stochastic (DSM) neuron model and its formalism. In chapter 4, I focus on the experiment done, approaches and results. The main conclusion drawn from the results gained is presented in Chapter 5.

Chapter 2

THE STRUCTURE AND ELECTRICAL ACTIVITY OF NEURONS

2.1 Neuron Structure and Morphology

Neurons are main building blocks of the brain that highly specialized for generating electrical signals in response to chemical and other inputs, and transmitting them to other cells. These cells have a sort of morphological specializations like dendrite and axon. Dendrites receive inputs from other neurons and propagate it to the main body of neuron cell called soma. The axon then carries the neuronal output to other cells. The branching structure of the dendritic tree increases surface area of the cell enhancing the ability of neuron to receive inputs from many other neurons through synaptic connections. Fig. 2.1 shows structure and information flow in a schematic neuron. Axons from single neurons can traverse large fractions of the brain or, in some cases, of the entire body. In the mouse brain, it has been estimated that cortical neurons typically send out a total of about 40 mm of axon and have approximately 4 mm of total dendritic cable in their branched dendritic trees. The axon makes an average of 180 synaptic connections with other neurons per μm of length while the dendritic tree receives, on average, 2 synaptic inputs per μm. The cell body or soma of a typical cortical neurons ranges in diameter from about 10 to 50 μm. (Dayan Abbot 2002)

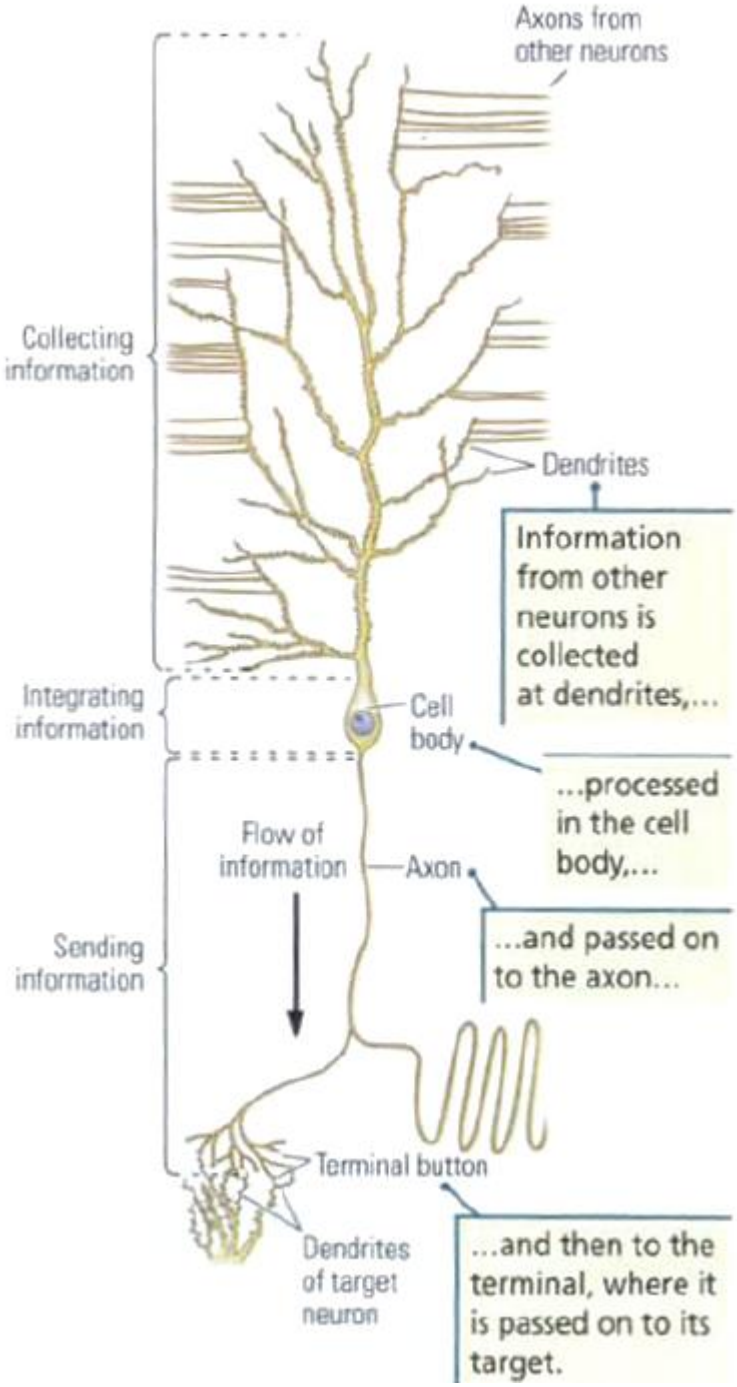

Figure 2.1: Information Flow in a Neuron (Kolb and Whishaw 2009).

2.1.1 Membrane Proteins

Proteins embedded in the cell membrane transport substances across it. Knowing something about how membrane proteins work is useful for understanding many functions of neurons. We describe three categories of membrane proteins that assist in transporting substances across the membrane. In each case, the protein's function is an emergent property of its shape or its ability to change shape. The categories are channels, gates, and pumps.

2.1.1.1 Channels

Some membrane proteins are shaped in such a way that they create channels, or holes, through which substances can pass. Different proteins with different-sized holes allow different substances to enter or leave the cell. Protein molecules serve as channels for predominantly sodium (Na+), potassium (K+), calcium (Ca2+), and chloride (Cl−) ions.

2.1.1.2. Gates

An important feature of some protein molecules is their ability to change shape. Some gates work by changing shape when another chemical binds to them. In these cases, the embedded protein molecule acts as a door lock. When a key of the appropriate size and shape is inserted into it and turned, the locking device changes shape and becomes activated. Other gates change shape when certain conditions in their environment, such as electrical charge or temperature, change.

2.1.1.3. Pumps

In some cases, a membrane protein acts as a pump, a transporter molecule that requires energy to move substances across the membrane. For instance, there is a

protein that changes its shape to pump Na+ ions in one direction and K+ ions in the other direction. Many substances are transported by protein pumps.

Channels, gates, and pumps play an important role in a neuron's ability to convey information.

2.1.2 Synapse

Synapses are shaped in the form of a junction between two successive neurons when the axon of afferent neuron is connected to the efferent one and provides a way to convey the information to other cell. Axons terminate at synapses where the voltage transient of the action potential opens ion channels producing an influx of Ca2+ that leads to the release of a neurotransmitter. The neurotransmitter binds to receptors at the signal receiving or postsynaptic side of the synapse causing ion-conducting channels to open. Depending on the nature of the ion flow, the synapses can have either an excitatory, depolarizing, or an inhibitory, typically hyperpolarizing, effect on the postsynaptic neuron (Dayan and Abbot 2002).

Synapses are not randomly distributed over the dendritic surface. In general, inhibitory synapses are more proximal than excitatory synapses, although they are also present at distal dendritic regions and, when present, on some spines in conjunction with an excitatory input (Segev in Bower and Beeman 2003). In many systems (e.g., pyramidal hippocampal cells and cerebellar Purkinje cells), a given input source is preferentially mapped onto a given region of the dendritic tree (Shepherd 1990), rather being randomly distributed over the dendritic surface. Electron micrographic images of synapses in real neurons are shown in fig. 2.2.

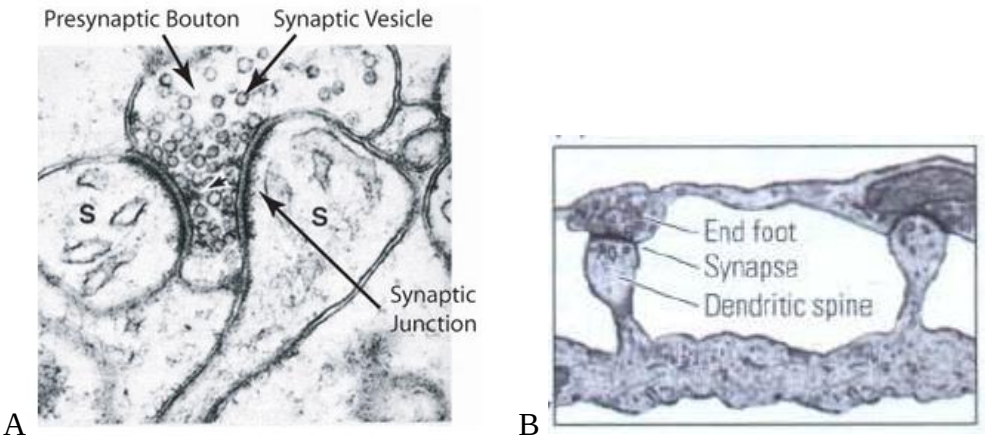

Figure 2.2: Examples of synapses. (A) Electron micrograph of excitatory spiny synapses (s) formed on the dendrites of a rodent hippocampal pyramidal cell. (B) An electron micrographic image capture the synapse formed where the terminal button of one neuron meets a dendritic spine on a dendrite of another neuron (Kolb and Whishaw 2009).

2.2 Membrane Potential and Neuron Electrical Activity

Membrane potential is defined as difference in electrical potential between the interior of a neuron and the surrounding extracellular fluid. Under resting conditions, the potential inside the cell membrane of a neuron is about -70 mV relative to that of the surrounding bath. This voltage, however, is conventionally assumed to be 0 mV for convenience and the cell is said to be polarized in this state. This potential is an equilibrium point at which the flow of ions into the cell matches that out of the cell. This membrane potential difference is sustained by ion pumps located in the cell membrane by maintaining concentration gradients. For example, Na+ is much more concentrated outside a neuron than inside it, and the concentration of K+ is significantly higher inside the neuron than in the extracellular fluid. Therefore, ions flow into and out of a cell due to both voltage and concentration gradients throughout the state transition of cell. Current, in the form of positively charged ions flowing out

of the cell (or negatively charged ions flowing into the cell) through open channels makes the membrane potential more negative, a process called hyperpolarization. Current flowing into the cell changes the membrane potential to less negative or even positive values. This is called depolarization. When a neuron is depolarized sufficiently large to raise the membrane potential above a threshold level, a positive feedback process is started, and the neuron generates an action potential. An action potential is a roughly 100 mV fluctuation in the electrical potential across the cell membrane that lasts for about 1ms. Once an action potential takes place it may be impossible to initiate another spike right after the previous one and this is called the absolute refractory period. The importance of action potential is that unlike subthreshold fluctuations that attenuate over distance of at most 1 millimeter they can propagate over large distances without attenuation along axon processes (Dayan and Abbot 2002). Figure 2.3 depicts the voltage dynamic of a neuron during an action potential while it is synthesized by corresponding ion channel activities throughout an action potential. In this figure the resting potential is in its real value -70 mV.

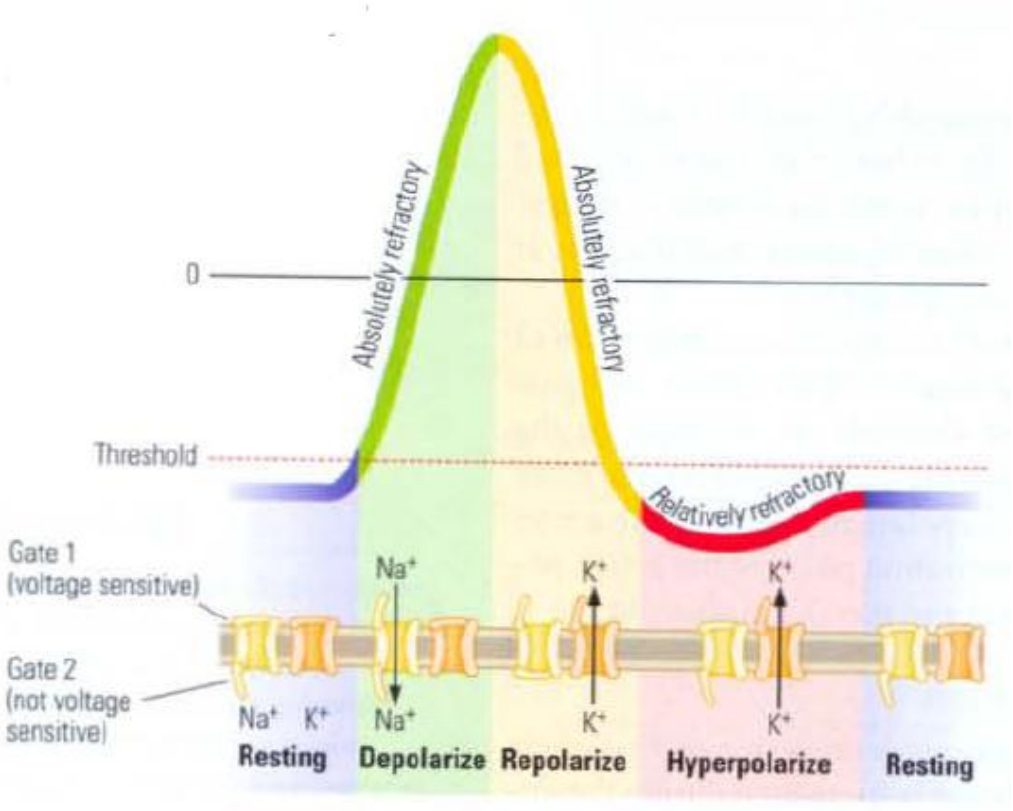

Figure 2.3: Phases of an Action Potential Initiated by changes in voltage sensitive sodium and potassium channels, an action potential begins with a depolarization (gate 1 of the sodium channel opens and then gate 2 closes). The slower-opening potassium channel contributes on repolarization and hyperpolarization until the resting membrane potential is restored (Kolb and Whishaw 2009).

Chapter 3

MODELING NEURAL EXCITABILITY

3.1 Introduction

Throughout the years, many neuronal models have been developed for different purposes. These models vary from structurally realistic biophysical models, like the Hodgkin-Huxley (HH) model, to simplified models, like Hindmarsh-Rose (HR) model that is mostly used in studying synchronization theories in large ensembles of neurons. In various studies, different models may be used depending on biological features of models, their complexity and the costs of implementation. Nevertheless, methods of modeling neural excitability have been significantly influenced by the landmark work of Hodgkin and Huxley (1952).

In this chapter I present a brief overview of Hodgkin-Huxley and Hindmarsh-Rose model. Afterward, I turn your attention to a recent physically inspired dissipative stochastic mechanics based neuron model that yields the dynamics of Hindmarsh-Rose model in deterministic state on which the study and experiment has been conducted.

3.2 The Hodgkin-Huxley Model

Based on experimental investigation on giant squid axon using space clamp and voltage clamp techniques, Hodgkin and Huxley (1952) could demonstrate that the current flowing across the squid axon membrane had only two major ionic components, I_{Na} and I_K (sodium channel and potassium channel equivalent components). These currents were strongly influenced by membrane potential V_m.

They consequently developed a mathematical model of their observation to make a model which is still most significant one based on which many realistic neural models have been developed.

In their model, the electrical properties of a segment of nerve membrane can be modeled by an equivalent circuit in which current flow across the membrane has two major components, one associated with charging the membrane capacitance and one associated with the movement of specific types of ions across the membrane. The ionic current is further subdivided into three distinct components, a sodium current I_{Na}, a potassium current I_K, and a small leakage current I_L that is primarily carried by chloride ions.

The differential equation corresponding to the electrical circuit is as follows:

$$C_m \frac{dV_m}{dt} + I_{ion} = I_{ext},$$

where C_m is the membrane capacitance, V_m is the membrane potential, and I_{ext} is an externally applied current. I_{ion} is the ionic current flowing across the membrane and can be obtained from:

$$I_{ion} = \sum_i I_i,$$

$$I_i = g_i(V_m - E_i).$$

I_i here denotes each individual ionic component having an associated conductance g_i and reversal potential E_i.

In the squid giant axon model, there are three I_i terms: a sodium current I_{Na}, a potassium current I_K, and a leakage current I_L and results in the following equation:

$$I_{ion} = I_{Na} + I_K + I_L = g_{Na}(V_m - E_{Na}) + g_K(V_m - E_K) + g_L(V_m - E_L)$$

The macroscopic g_i (g_{Na}, g_K, g_L) conductances arise from the combined effects of a large number of microscopic ion channels in the membrane. Ion channel can be thought of as containing a small number of physical gates that regulate the flow of ions through the channel. In an ion channel when all of the gates are in the permissive state, ions can pass through the channel and the channel is open.

3.2.1 The Ionic Conductances

Ions can pass through the channel and the channel is open when all of the gates for a particular channel are in the permissive state. The formal assumptions used to describe the potassium and sodium conductances empirically achieved by voltage clamp experiments are:

$$g_K = \bar{g}_K n^4,$$

$$g_{Na} = \bar{g}_{Na} m^3 h,$$

where n, m and h are ion channel gate variables dynamics of which will be presented later on. $\bar{g}_i$ is a constant with the dimensions of conductance per cm^2 (recall that n is

between 0 and 1, therefore, we need the value of maximum conductance ($\bar{g}_i$) to normalize the result).

The dynamics of n, m and h are as follows:

$$\dot{n} = \frac{dn}{dt} = \alpha_n(1-n) - \beta_n n \tag{2.1}$$

$$\dot{m} = \frac{dm}{dt} = \alpha_m(1-m) - \beta_m m$$

$$\dot{h} = \frac{dh}{dt} = \alpha_h(1-h) - \beta_h h$$

where α_x and β_x are rate constants which vary with voltage but not with time, *n* is a dimensionless variable which can vary between 0 and 1 and represents the probability of an individual gate being in the permissive state.

In voltage clamp experiment the membrane potential starts in the resting state (V_m = 0) and is then instantaneously stepped to a new clamp voltage $V_m = V_c$. The solution to Eq.s (2.1) is a simple exponential of the form

$$x(t) = x_\infty(V_c) - (x_\infty(V_c) - x_\infty(0))\exp(-t/\tau_x),$$

$$x_\infty(0) = \alpha_x(0)/\alpha_x(0) + \beta_x(0),$$

$$x_\infty(V_c) = \alpha_x(V_c)/\alpha_x(V_c) + \beta_x(V_c),$$

$$\tau_x(V_c) = [\alpha_x(V_c) + \beta_x(V_c)]^{-1},$$

where x denotes time dependent gating variables n, m and h for simplicity of formulation, $x_\infty(0)$ and $x_\infty(V_c)$ are the value of gating variables at conventional resting state voltage 0 and clamped voltage V_c. τ_x denotes the constant time course for approaching the steady state value of $x_\infty(V_c)$ when the voltage is clamped to V_c.

Hodgkin and Huxley measured constants α_i, β_i as functions of V in the following form:

$$\alpha_i = \frac{x_\infty(V)}{\tau_n(V)},$$

$$\beta_i = \frac{1 - x_\infty(V)}{\tau_n(V)},$$

As mentioned earlier i is a representative for n, m, and h ion channel gate variables. Below are the expressions for the rate constants α_i and β_i that are empirically determined:

$$\alpha_n(V) = \frac{0.01(10 - V)}{\exp\left(\frac{10 - V}{10}\right) - 1},$$

$$\beta_n(V) = 0.125 \exp\left(-\frac{V}{80}\right),$$

$$\alpha_m(V) = \frac{0.1(25 - V)}{\exp\left(\frac{10 - V}{10}\right) - 1},$$

$$\beta_m(V) = 4 \exp\left(-\frac{V}{18}\right),$$

$$\alpha_h(V) = 0.07 \exp\left(-\frac{V}{20}\right),$$

$$\beta_h(V) = \frac{1}{\exp\left(\frac{30 - V}{10}\right) + 1}.$$

3.3 The Hindmarsh Rose Model

Although the Hodgkin-Huxley (HH) can describe neural dynamics of spiking neuron to a considerable extent, the bursting model of the HH can be complex in extensive models. Hodgkin-Huxley had studied the axon part of squid neuron containing Na and K conductance, whereas, more conductance types take part in the bursting model of the HH model which in part make the model more complicated.

FitzHugh and Nagumo observed independently that in the Hodgkin-Huxley equations, the membrane potential V(t) as well as sodium activation m(t) evolve on similar time-scales during an action potential, while sodium inactivation h(t) and potassium activation n(t) change on similar, although slower time scales. As a result, a model simulating spiking behavior can now be represented by the following equations

$$\dot{x} = a(y - f_1(x) + I), \qquad (3.1)$$

$$\dot{y} = b(g_1(x) - y)$$

where x denotes membrane potential and y is a recovery variable. $f_1(x)$ is a cubic function, $g_1(x)$ is a linear function, parameters a and b are time constants and I(t) is the external applied or clamping current as function of time t.

Hindmarsh and Rose made use of the FitzHugh-Nagumo model to develop their own model, which was more or less a simplification of the Hodgkin-Huxley equations and did replace the linear function g(x) with a quadratic function to makes the model capable of rapid firing with a long interspace interval. Fig. 1.1 shows the nullcline diagram for the 1982 Hindmarsh-Rose model.

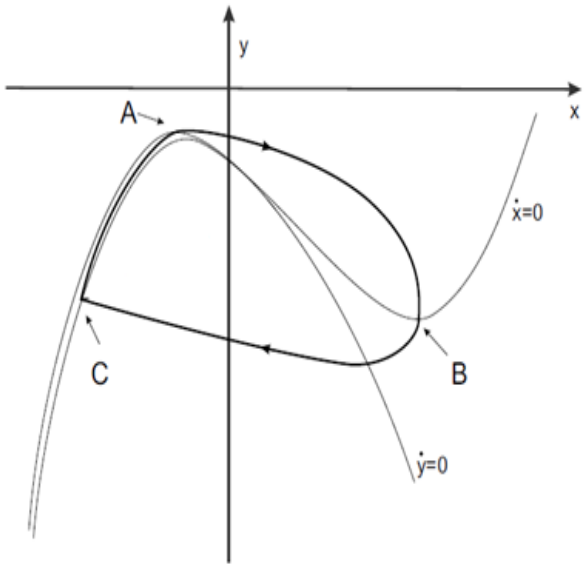

Figure 3.1: Phase plane analysis of the 1982 HR model. Nulclines x= 0, y= 0 (thin lines) and firing limit-cycle (thick line). The model has only one equilibrium point at this stage (Steur 2006).

More than one equilibrium point was required for the HR model to yield burst firing behavior; essentially one point for the subthreshold stable resting state and one point within the firing limit cycle. A slight deformation was required to make the nullclines to intersect and bring about additive equilibrium points. To meet the requirements the governing equations were changed to the following form:

$$\dot{x} = y - f(x) + I,$$

$$\dot{y} = g(x) - y,$$

where $f(x) = x^3 - 3x^2$ in the simple form of $f(x)$ in HR model, $g(x) = 1 - 5x^2$. The phase plane analysis of the given equations is shown in Fig. 3.2.

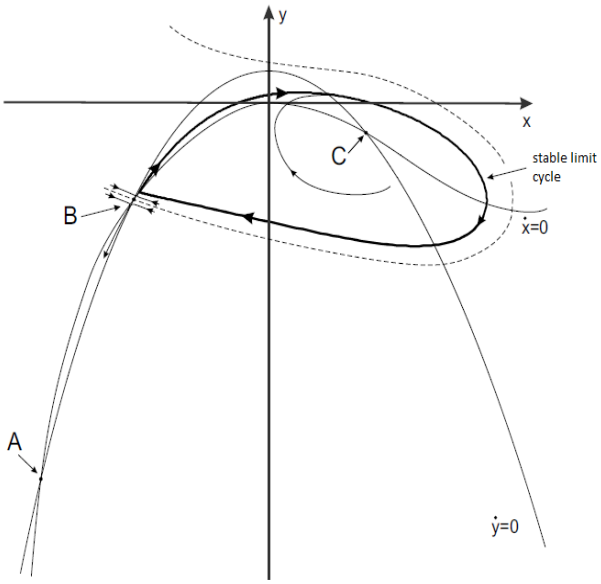

Figure 3.2: Phase plane representation of Rose Hindmarsh Model. The equilibrium points A, B and C are a stable node, an unstable saddle, and an unstable spiral, respectively. A simple form of f(x) is used in this equation as is shown $\dot{x} = 0$ nullcline shows (Steur 2006).

Point A in the diagram is a stable node which corresponds to the resting state of neuron. By applying a large enough depolarizing current pulse, the $\dot{x} = 0$ nulcline will be lowered such that the saddle point B and point A meet and finally vanish. From this point the state will rise up the narrow channel and enter a stable limit cycle. However, terminating of the firing is not possible by simply ending the stimulus and the state will only leave the limit cycle after a suitable hyperpolarizing pulse is applied. Consequently, the term z was added to the model so that it can terminate the model firing state. This additive variable represents a slowly varying current, changing the applied current I to the effective input I - z. The value of z needs to be raised when the neuron is in firing state. The general HR model's set of equations after this modification is as follows:

$$\dot{x} = -x^3 + 3x^2 + y + I - z,$$

$$\dot{y} = 1 - 5x^2 - y,$$

$$\dot{z} = r\,(h(x) - z)\,;$$

Note that the f(x) and g(x) have been replaced with their equivalents. In these equations x represents membrane potential, y is a recovery variable, and z represents the adaptation current with time constant r. variable z increases during the firing state and decreases during the non-firing state. Parameters h and r made the model capable of exhibiting bursting, chaotic bursting and post-inhibitory rebound. (Rose and Hindmarsh 1984; Steur 2006). Fig. 3.3 demonstrates the phase plane analysis of equation (3.2) using more complex form of f(x) as proposed in (Rose and Hindmarsh 1984).

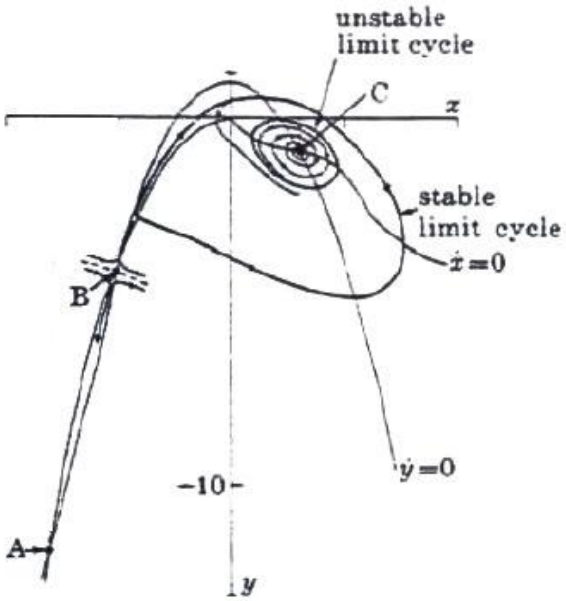

Figure 3.3: Phase plane representation of Rose Hindmarsh Model using a more complex form of f(x). The equilibrium points A, B and C are a stable node, an unstable saddle, and an unstable spiral, respectively. Unstable limit cycle is specified here (Rose and Hindmarsh 1984).

3.4 The DSM Neuron Model

The distinctive formulation of the Dissipative Stochastic Mechanics based (DSM) neuron stems from a viewpoint that conformational changes in ion channels are exposed to two different kinds of noise. These two kinds of noise were coined as the intrinsic noise and topological noise. The intrinsic noise arises from voltage dependent movement of gating particles between the inner and the outer faces of the membrane which is stochastic; therefore, gates open and close in a probabilistic fashion, that is, it is the average number, not the exact number, of open gates over the membrane is specified by the voltage.

The topological noise, on the other hand, stems from the presence of a multiple number of gates in the channels and is attributed to the fluctuations in the topology of open gates, rather than the fluctuations in the number of open gates.

Curiously, since gating particles, throughout the dynamics, do not follow a prescribed order in occupying the available closed gates, and in vacating the open gates, the membrane at two different times may have the same number of open gates but two different conductance values. The topological noise is attributed to the uncertainty in the number of open channels that takes place even if the number of open gates is exactly known. Hence, in determining the voltage dynamics, all the permissible topologies of open gates should be respected. Formalism of the DSM neuron was developed using the Rose–Hindmarsh model (Hindmarsh and Rose 1984) and makes use of the Nelson's stochastic mechanics (Nelson 1966 and 1967), in the presence of dissipation, for modeling the effects of ion channel noise on voltage dynamics of the membrane. The effect of the topological noise on the

dynamics of the neuron becomes more significant in smaller membrane sizes. Therefore in too large neurons the DSM neuron behaves as the Hindmarsh-Rose model does.

The DSM neuron formalism yields the equations of motion for both first and second cumulants of the variables. The second cumulants, which describe the neuron's diffusive behavior, do not concern us in the current thesis. First cumulants evolve in accordance with the following dynamics:

$$m\dot{X} = \Pi + S_5 I$$

$$\dot{\Pi} = -\left(\frac{3a}{m}X^2 - \frac{2b}{m}X + S_0\right)(\Pi + S_5 I) - S_1 a X^3 + S_2 X^2 + S_6 X - S_3 X_{eq}(I) +$$

$$S_1 I + S_7 - (1-r)\left[k\left(1 - \frac{\varepsilon_m^y}{m}\right)z + (1-k)\left(1 - \frac{\varepsilon_m^z}{m}\right)y\right]$$

$$\dot{y} = -y - dX^2 + c + \eta^y \tag{3.1}$$

$$\dot{z} = -rz + rh(X - x_s) + \eta^z \tag{3.2}$$

$$\Pi(t_0) = y(t_0) - z(t_0) - a\big(X(t_0)\big)^3 + b\big(X(t_0)\big)^2 + (1 - S_5)I(t_0) \tag{3.3}$$

where *X* denotes the expectation value of the membrane voltage, and Π corresponds to the expectation value of a momentum-like operator. The auxiliary variables *y* and *z* represent the fast and the slower ion dynamics, respectively. *I* denotes the external current injected into the neuron, and *m* denotes the membrane capacitance. The parameters *a*, *b*, *c*, *d*, *r*, and *h* are some constants. *k* is a mixing coefficient given by *k = 1/(1+r)*. S_js are some constants as follows:

$$S_0 := k + (1-k)r,$$

$$S_1 := S_0 - \left[k\frac{\varepsilon_m^y}{m} + (1-k)r\frac{\varepsilon_m^z}{m}\right],$$

$$S_2 := k\left(1 - \frac{\varepsilon_m^y}{m}\right)(b-d) + (1-k)\left(1 - \frac{\varepsilon_m^z}{m}\right)(rb-d),$$

$$S_3 := k\varepsilon_u^y + (1-k)\varepsilon_u^z,$$

$S_4 := k\frac{\varepsilon_m^y}{m} + (1-k)\frac{\varepsilon_m^z}{m},$

$S_5 := 1 - S_4,$

$S_6 := S_3 - S_5 rh,$

$S_7 := (rhx_s + c)S_5.$

Eq. (3.3) specifies the value of Π at the initial time t_0 in terms of the initial values of the other dynamical variables *X*, *y* and *z*, and the current *I*. $X_{eq}(I)$ obeys the equation

$aX_{eq}^3 - (b-d)X_{eq}^2 + h(X_{eq} - x_s) - c - I = 0$

where x_s is a constant. η^y and η^z in Eqs. (3.1) and (3.2) are Gaussian white noises with zero means and mean squares given by

$< \eta^y(t)\eta^y(t') >= 2mT\delta(t-t')$

and

$< \eta^z(t)\eta^z(t') >= 2rmT\delta(t-t')$

were obtained by means of the classical fluctuation-dissipation theorem. T here is a temperature-like parameter. The terms with the *correction coefficients* $\varepsilon_m^y, \varepsilon_u^y, \varepsilon_m^z$ and ε_u^z that take place in the above equations are the renormalization terms.

When the noise terms η^y, η^z are ignored and all the correction coefficients are set to zero, the DSM dynamics becomes equivalent to the Rose-Hindmarsh dynamics. All the parameters of the model, including time, are in dimensionless units. The original membrane voltage time series for Hindmarsh-Rose original model is for some various constant input currents are shown in the Fig. 3.4. Dynamical states of the Rose–Hindmarsh model are quiescence, bursting (rhythmic with a high degree of periodicity, or chaotic), and tonic firing.

Güler (2008) showed that the role played by the intrinsic noise, becomes more significant in smaller size of the membranes (or, equivalently, fewer channels) in DSM Neuron. The intrinsic noise can cause spiking activity in otherwise quiet deterministic model and results in bursting in larger input current values. The dynamics of DSM Neuron in a relatively smaller size of membrane is displayed in fig. 3.5. Note that renormalization corrections have been set to zero so that the result is observed regardless of the topological noise effect.

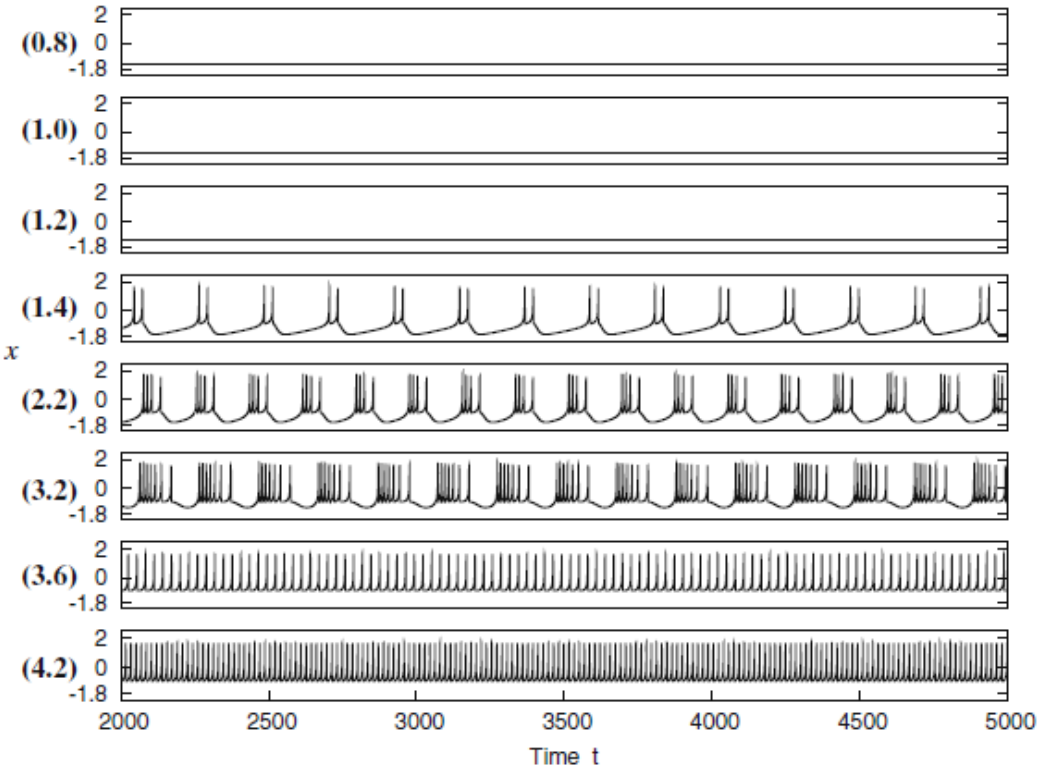

Figure 3.4: Membrane voltage time series of the deterministic Rose–Hindmarsh model using the parameter values m = 1, a = 1, b = 3, c = 1, d = 5, h = 4, r = 0.004 and $x_s = -1.6$; for various constant input current values I, indicated in parenthesis on the left of each plot (Güler 2008).

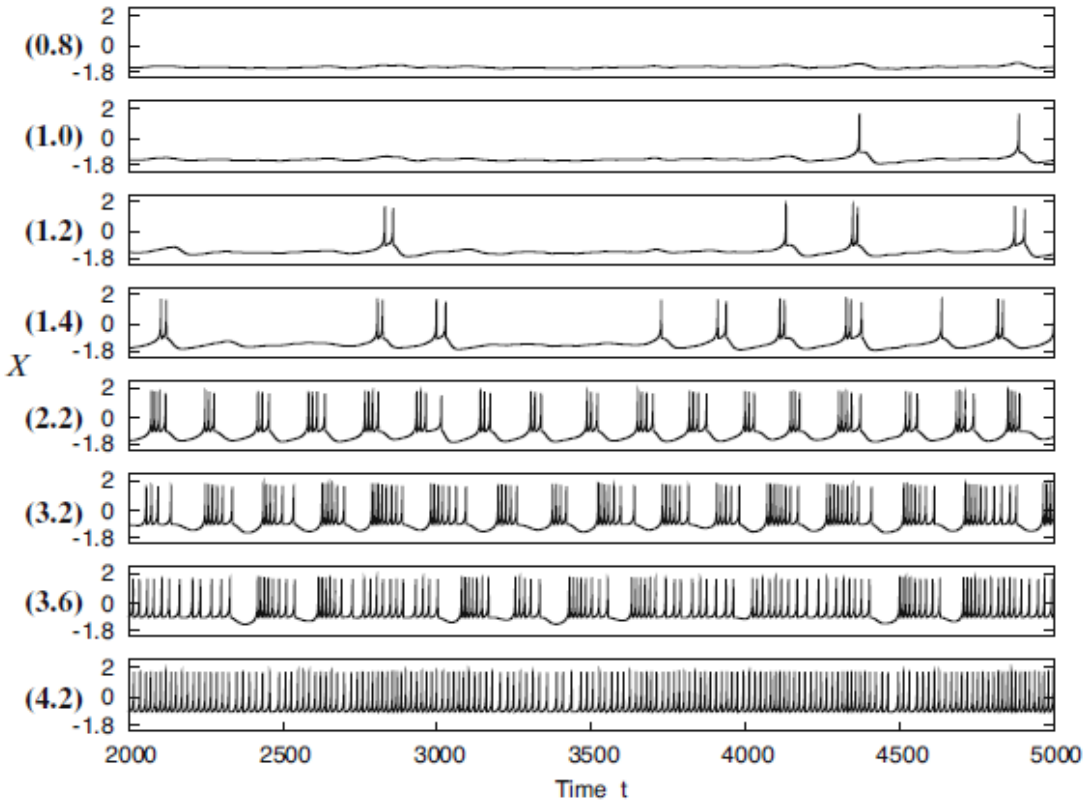

Figure 3.5: Time series of X when the DSM neuron is subjected to the intrinsic noise only using the Rose–Hindmarsh parameter values $m = 0.25$, $a = 0.25$, $b = 0.75$, $c = 0.25$, $d = 1.25$, $h = 1$, $r = 0.004$ and $x_s = -1.6$ with the temperature $T = 2$. Plots for various constant input current values $4I$ (scaled by the factor of four) (Güler 2008).

The renormalization corrections are induced by the mutual interaction between the topological noise and the intrinsic noise. Presence of the correction terms also increment further the behavioral transitions from quiescence to spiking and from tonic firing to bursting to a considerable extent and, consequently, lead to the bursting activity to take place in a wider range of input currents. i.e., with the presence of the correction terms, the spiking activity starts to take place at smaller input current values, and the bursting activity is prolonged for higher input current values. The behavior of DSM neuron under the influence of corrections is demonstrated in fig 3.6.

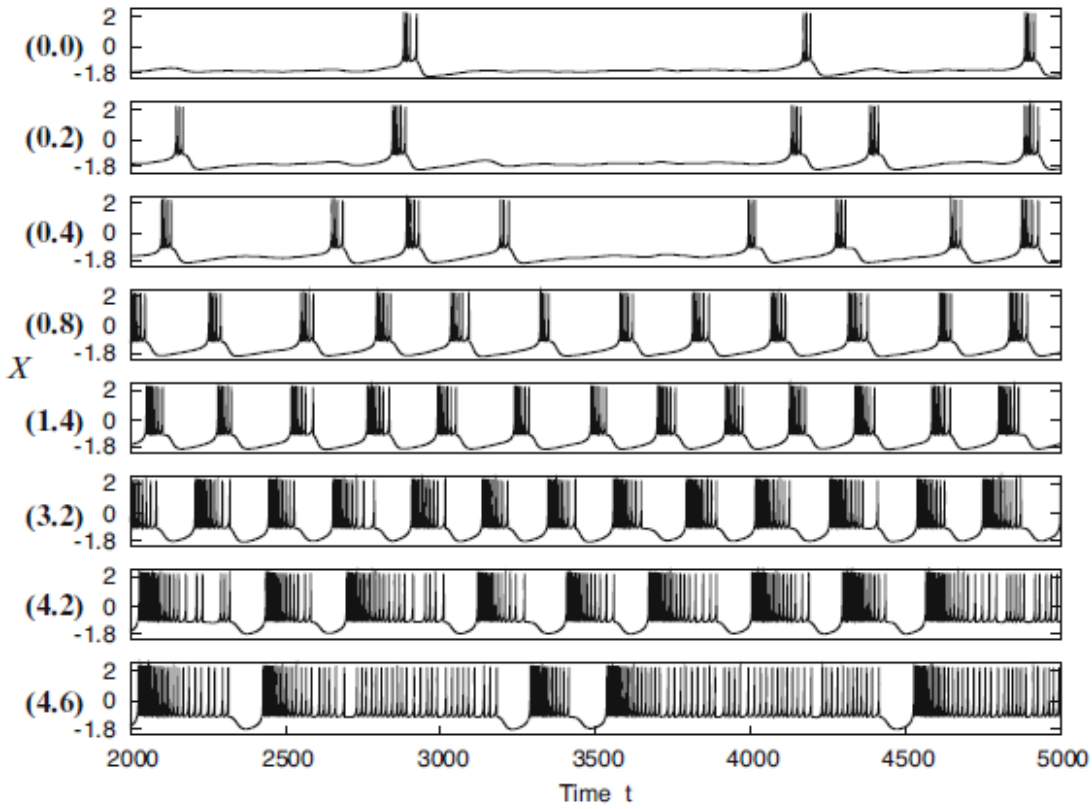

Figure 3.6: Time series of X using the correction coefficients $\varepsilon_m^y = 0.1$, $\varepsilon_u^y = 1.0$, $\varepsilon_m^z = 0.001$ and $\varepsilon_u^z = 0.005$ with the temperature T = 2. The Rose–Hindmarsh parameter values are m = 1, a = 1, b = 3, c = 1, d = 5, h = 4, r = 0.004 and $x_s = -1.6$ (Güler 2008).

Chapter 4

NOISE AND STOCHASTIC RESONANCE

4.1 Noise and Stochastic Resonance in Neuronal Information Processing

Noise can improve the signal transmission properties of neuronal systems under certain circumstances. Subthreshold oscillations in neuron can have a significant impact on the coding of information in neurons when are amplified by noise (Braun et al. 1997, 1998). The presence of an optimum amount of noise in the neuron system can be in cooperation with the input signal to improve the detection of the signal. In most cases there is an optimum for the noise amplitude which has motivated the name stochastic resonance for this rather counterintuitive phenomenon (Gerstner and Kistler 2002).

Experimental and theoretical investigations have confirmed the presence of the Stochastic Resonance (SR) phenomenon in a single neuron, network of neurons and even in the scope of brain (Kitajo et al 2003; Ward et al. 2002).

Andreas T. Schaefer et al. (2006) using a combination of in vivo, in vitro, and theoretical approaches have shown that both synaptically and intrinsically generated membrane potential oscillations dramatically improve action potential (AP) precision by removing the membrane potential variance associated with jitter-accumulating trains of APs.

It has been shown that neuron ion channels which contribute to internal noise in neurons, can exhibit SR (Bezrukov and Vodyanov 1995). Synaptic noise in a stochastic network can amplify signal detection in CA1 neurons of hippocampus. It has been suggested that SR contributes in detection of tactile stimuli in the somatosensory system of cats, (Manjarrez et al. 2003). In addition, Jaramillo and Wiesenfeld (2000) stipulated that presence of optimal level of noise in the auditory system reveals that the system is tuned to take advantage of SR.

SR was put forward by Longtin et al. (1991) theoretically in neuron models. Dependence of SR on the input signal shape was studied by Lee et al. (1999) in the Hodgkin-Huxley (HH) model. In other studies exhibition of SR in HH models of pyramidal neuron cells was shown (Rudolph and Destexhe 2001a, 2001b).

SR also appears in simpler neuronal models such as Hindmarsh-Rose (HR) model of burst firing neurons the FitzHugh-Nagumo (FHN) model of tonic firing (Gong and Xu 2001; Lindner and Schimansky-Geier 1999, 2000). The role of on input signal and noise parameters was studied in the FHN model as we will do so with the DSM neuron model. Wang et al. (2000) found that SR increases selectivity for particular signal frequencies in HR neuron model that can in turn contribute in special information processing purposes.

4.2 Measuring Stochastic Resonance

Various approaches have been employed in order for neuronal Stochastic Resonance (SR) to be measured. Diversity of neuron models under study on one hand and the various properties of the stimulation on the other hand make neuron SR measurements distinctive. Consequently, recent studies have been done for SNR

computation having diverse methodologies for SNR computation over different neuron models.

The response of neuron to transient input subthreshold pulses has been studied over stochastic Hodgkin-Huxley neuron by Chen et al. (2008). They experimentally showed that channel noise enables one neuron to detect the subthreshold signals and an optimal membrane area exists for a single neuron to achieve optimal performance by computing the SNR. They made use of a proposed SNR formulation as the ratio of increased firing probability in response to input pulses to the probability for spontaneous firing in response to channel noise in order to find the range in the membrane area which is more sensitive to a pulse than the channel noise perturbation.

In another study, how internal noise stemming from individual ion channels does affect collective properties of the whole ensemble is investigated. The SNR in the study above is given by the ratio of signal peak height to the background height (Schmid et al. 2001).

Steafan Reinker et al. (2003) studied a stochastic Hindmarsh–Rose model using Monte-Carlo simulations. In this study the SNR has been computed upon stimulation of the neuron by a sinusoidal wave. They hold that extraneous action potentials appear in the spike train, implying that the neuron fires due to the noise level and not to the periodic sine wave stimulation. Therefore, the following is the general formula used for SNR computation as a measure of the correlation between the input signal and the output spike train (note that the input period here corresponds to the input sign wave period that results in spiking):

$$SNR = 10 \log_{10} \left[\frac{\#\ of\ spikes\ near\ input\ period}{total\ \#\ of\ spikes} \right].$$

SNR computation and optimization in auditory neurons, also, has been put forward by (Svirskis et al. 2002).

Stochastic resonance (SR) can be envisioned as a particular problem of signal extraction from background noise (Gammaitoni et al. 1998). It describes the amplification of weak signals in nonlinear systems in a coherent manner. In neurons, we know that the presence of ion channel noise can give rise to stochastic resonance (Bezrukov and Vodyanoy 1995; Jung and Shuai 2001, Schmid et al. 2001). Typically, SR is measured by the ratio of signal peak height to the background height, referred to as the signal-to-noise ratio (SNR).

Chapter 5

NUMERICAL EXPERIMENTS

5.1 The Approach for Signal-to-Noise Ratio Computation

In this study our aim is to examine the possible effect of the renormalization terms on SNR, using periodic input currents. As such, SNR is measured by the following formula:

$$SNR = \frac{A_i}{CV(d)}$$

where A_i is the amplitude of the input current, $CV()$ is the coefficient of variation; d is defined as either inter-bursting time interval (the distance between two sequential bursts) when the activity phase is bursting, or inter-spike time interval (the distance between spikes) when the activity phase is tonic firing. The coefficient of variation used in the formula is defined as $CV(d) = \frac{Var(d)}{\mu}$, in which, $Var(d)$ corresponds to the variance of d and μ is the mean value of d.

5.2 The Role Played by the Renormalization Correction in SNR

Instead of examining the role of the correction coefficients individually, we take the typical values as follows ($\varepsilon_m^y = 0.1,\ \varepsilon_u^y = 0.5,\ \varepsilon_m^z = 0.001,\ \varepsilon_u^z = 0.005$) and scale them by an overall coefficient $\varepsilon\text{-}coef$ to obtain a benchmark of different sets of correction coefficients. For example, if $\varepsilon\text{-}coef = 2$ that means the correction coefficients have the values ($\varepsilon_m^y = 0.2,\ \varepsilon_u^y = 1.0,\ \varepsilon_m^z = 0.002,\ \varepsilon_u^z = 0.01$). We apply the following periodic input current to the neuron:

$$I = I_{base} + A_i \sin(2\pi F_i\, t)$$

Here, I_{base} is the base current, A_i is the amplitude of the current oscillations, and F_i is the frequency of the input signal.

It is seen from figs. 5.1 and 5.2 that the presence of renormalization corrections makes the neuron become more excitable; the renormalization terms enhance spiking by increasing the number of spikes. The time course up to 1000 is not included in the figure to skip the transient activity.

The model's behavior is studied, in the context of SNR, within the following ranges of the parameters: $\varepsilon\text{-}coef \in (0 - 5)$; T $\in (0.008 - 0.020)$; $I_{base} \in (0 - 1.6)$; $A_i \in (0.3 - 0.8)$; $F_i \in (0.001 - 0.010)$. Confined to these ranges, average SNR values are computed using a set of 30000 samples over the parameter space $(T, \varepsilon\text{-}coef, I_{base}, A_i, F_i)$. The experiments involve not just a single value of SNR; but instead computations of various averages of SNR as a function of one of the five parameters, for instance$SNR(T|\, \varepsilon\text{-}coef, I_{base}, A_i, F_i)$ denotes the average SNR value as a function of T while employing the parameter space averaging over the other parameters $(\varepsilon\text{-}coef, I_{base}, A_i, F_i)$. In the experiments, the time course of stimulation was kept as large as 50000 to obtain a reliable accuracy in the results (In the figures, hoever, the time corse is set to 5000 in order for the voltage tiem series to be observable by the reader). Figs. 5.3 and 5.4 display the computed SNR averages. The main observation is that SNR increases with the correction coefficients up to a saturation value. Thus the renormalization terms cause a profound rise in SNR. At the saturation state the SNR would not raise up further due to the model that does not yield spike any more by setting higher values to correction coefficients.

The optimum values of the concerned parameters that result in the highest and the lowest SNR are of concern. We have given the voltage time series in fig. 5.5 for those parameter sets that yield the worst and the best SNR.

5.3 Technologies Used

The DSM neuron model has been developed by Prof. Marifi Güler and I added some modifications to make the experiments possible.

From technological point of view the model has been developed by C++ programming language. I have made use of GnuPlot for the results and voltage time series to be plotted. The experiments have been conducted concurrently over 50 workstations.

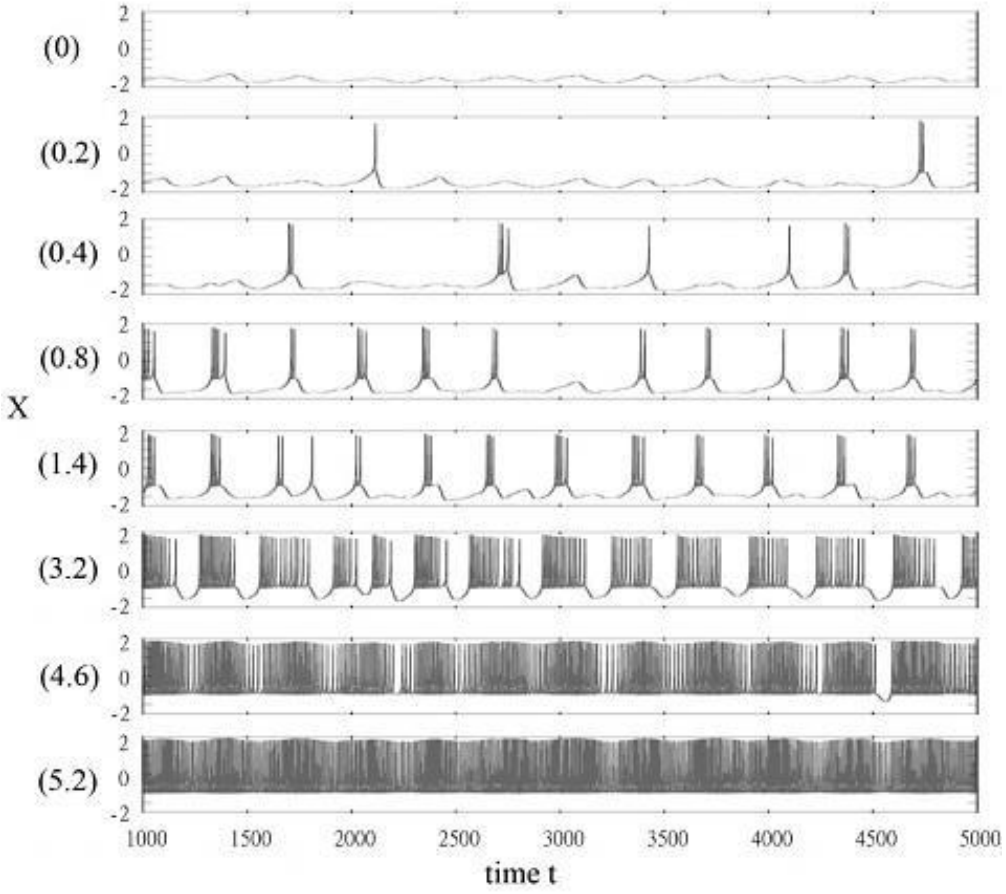

Figure 5.1: Time series of X using $T = 0.016$. The Rose-Hindmarsh parameter values are $m = 1, a = 1, b = 3, c = 1, d = 5, h = 4, r = 0.004$ and $x_s = -1.6$. Time varying input current parameter values are $A_i = 0.003, F_i = 0.005$; respective I_{base} values are represented within parenthesis for each particular plot. Correction coefficients: $\varepsilon_m^y = 0$, $\varepsilon_u^y = 0$, $\varepsilon_m^z = 0$ and $\varepsilon_u^z = 0$ ($\varepsilon\text{-}coef = 0$)

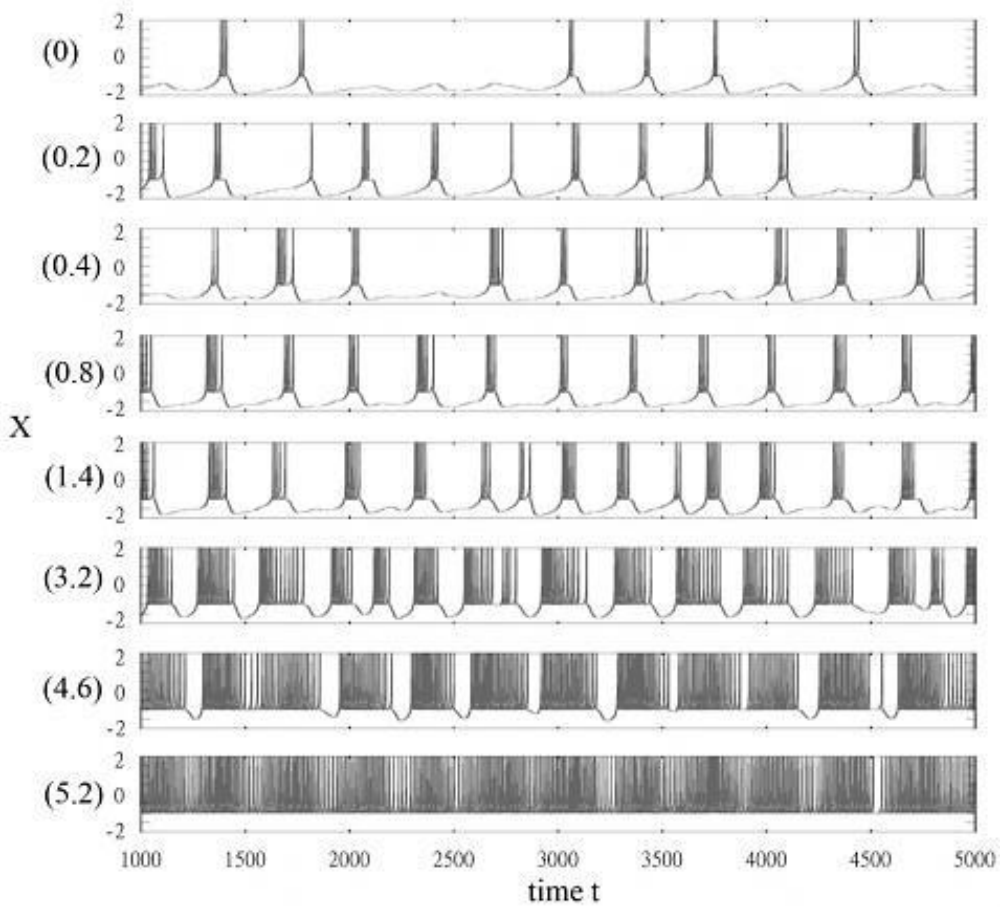

Figure 5.2: Time series of X using $T = 0.016$. The Rose-Hindmarsh parameter values are $m = 1, a = 1, b = 3, c = 1, d = 5, h = 4, r = 0.004$ and $x_s = -1.6$. Time varying input current parameter values are $A_i = 0.003, F_i = 0.005$; respective I_{base} values are represented within parenthesis for each particular plot. Correction coefficients: $\varepsilon_m^y = 0.1$, $\varepsilon_u^y = 0.5$, $\varepsilon_m^z = 0.001$ and $\varepsilon_u^z = 0.005$ ($\varepsilon\text{-}coef = 1$)

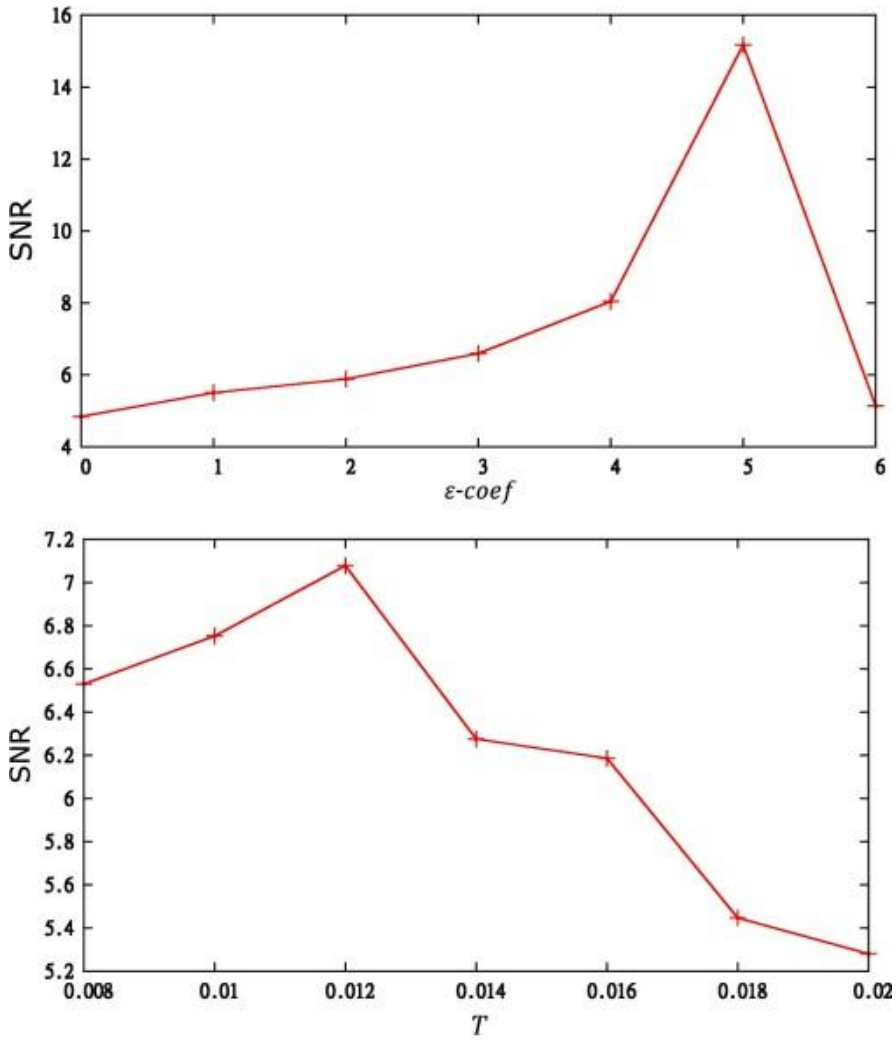

Figure 5.3: SNR mean values in terms of specific parameters $\varepsilon\text{-}coef$ and T. The means were computed using a set of 30000 samples over the parameter space $(T, \varepsilon\text{-}coef, I_{base}, A_i, F_i)$ SNR against model parameters $\varepsilon\text{-}coef$ and T. $SNR(\varepsilon\text{-}coef|T\ , I_{base}, A_i, F_i)$ and $SNR(T|\varepsilon\text{-}coef\ , I_{base}, A_i, F_i)$ are plotted. Each SNR mean value corresponds to the result of the average obtained from 30000 experiments. Stimulation time for each experiment is 50000.

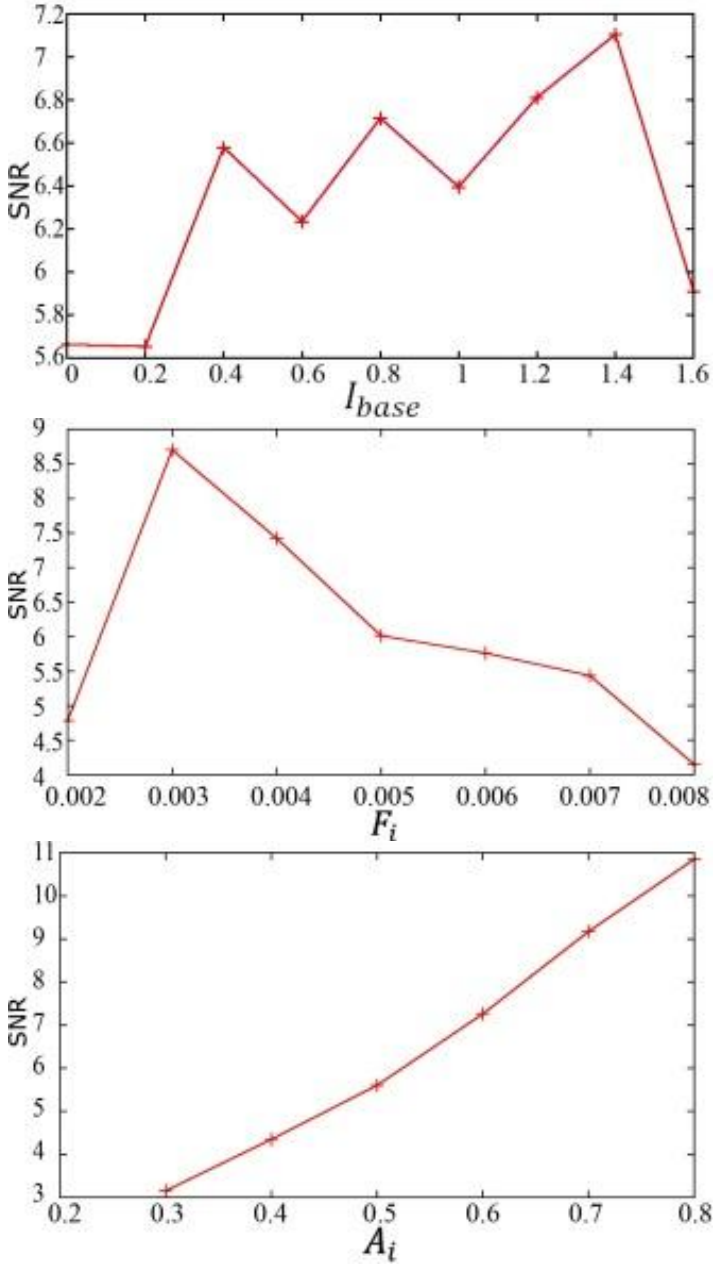

Figure 5.4: SNR mean values in terms of specific parameters , $I_{base}, A_i,$ and F_i. The means were computed using a set of 30000 samples over the parameter space $(T, \varepsilon\text{-}coef, I_{base}, A_i, F_i)$. SNR against input signal parameters I_{base}, F_i, and A_i. $SNR(I_{base}, |T, \varepsilon\text{-}coef\ , A_i, F_i)$, $SNR(F_i|T\ , \varepsilon\text{-}coef, I_{base}, A_i)$, and $SNR(A_i|T, \varepsilon\text{-}coef\ , I_{base}, F_i)$ are plotted. Each SNR mean value corresponds to the result of the average obtained from 30000 experiments. Stimulation time for each experiment is 50000.

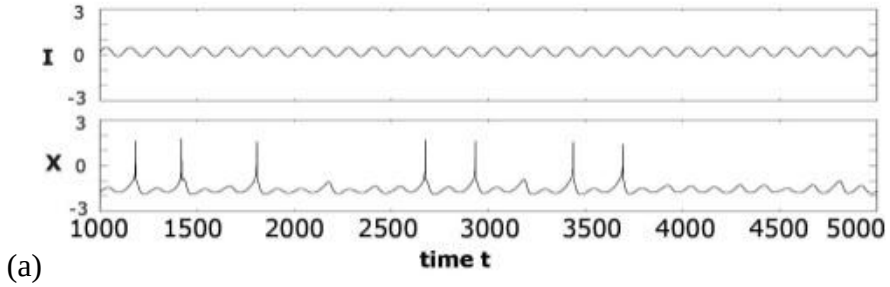

(a)

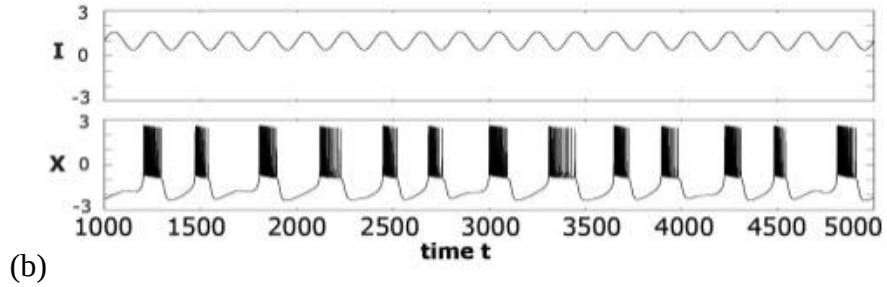

(b)

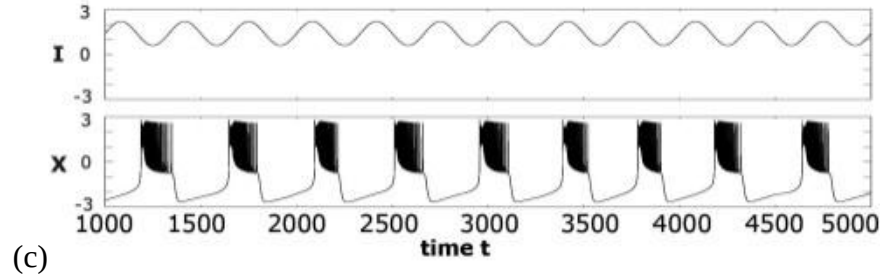

(c)

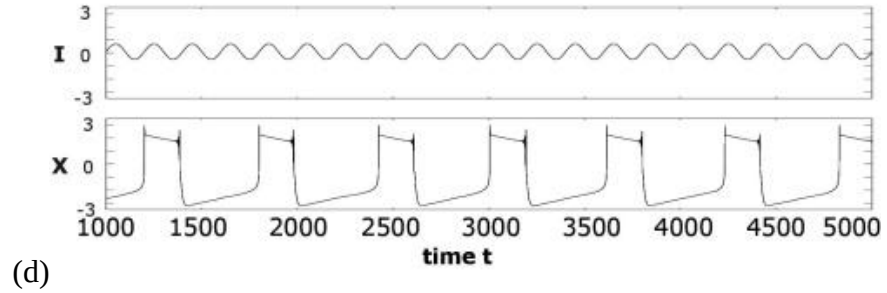

(d)

Figure 5.5: Input current I and the voltage x are plotted in time using: (a) Least efficient parameter values: T =0.02, $\varepsilon\text{-}coef$ =0, I_{base}=0.2, A_i=0.3, F_i=0.008. (b) Mid efficient parameter values: T =0.016, $\varepsilon\text{-}coef$ =3, I_{base}=1, A_i=0.6, F_i=0.005. (c) Most efficient parameter values: T =0.012, $\varepsilon\text{-}coef$ =4, I_{base}=1.4, A_i=0.8, F_i=0.003. (d) Saturation state: the set of parameter values are the same with mid efficient values except that ε-coef =5.

Chapter 6

CONCLUDING REMARKS

In this Thesis, we studied the DSM neuron model numerically when subjected to a periodic input current. The role of the renormalization corrections was inspected in the context of signal-to-noise ratio. Correction coefficients were used as a magnitude for the efficiency of renormalization corrections in the model. Recall that these renormalization corrections stem from the uncertainty in the number of open ion-cannels even if the number of permissible gates is exactly known.

The DSM neuron model might seem to be more complicated than the counterparts. Exposing faster synchronization between two DSM neurons (Jibril and Güler, 2009), the model's dynamics under constant input currents (Güler, 2008) and also its capability in signal detection under time varying periodic input currents which was investigated in this study are all the advantages of this model that worth bearing its complexity. Moreover, it should be taken into account that this model is highly capable of modeling the neurons in smaller membrane sizes.

Based on the experiments' results, the SNR raises up by incrementing the correction coefficients values up to the saturation state of the model in which the correction coefficients cannot be increased further. The amplitude of the input signal has expectedly profound effect on SNR. Having that in mind, interestingly, the

significance of the effect of renormalization corrections is comparable to that of amplitude of the input current.

It was found that the renormalized equations of activity give a significantly higher SNR value and consequently the exhibition of the Stochastic Resonance phenomenon is observed. The superiority of the DSM model against the deterministic models has been demonstrated earlier [2]. In this study, however, we showed that the DSM model also yields higher SNR in comparison to the stochastic models which solely make use of stochastic differential equations obtained by introducing some white noise terms of vanishing means into the underlying deterministic equations. That is to say, it turns out from the numerical experiments that the mean value of SNR becomes higher in DSM neuron in which the interaction of topological noise and intrinsic noise is taken into account than the Rose-Hindmarsh model having incorporated merely the intrinsic noise. The number of samples in the experiment is as large as 30000 and the time course of stimulation in each sample is set to 50000 to gain a reliable and accurate result.

Since the model has been studied earlier under constant input currents, the time varying characteristic of the input current is of our concern. The input current is periodic having no noise applied on it. Perhaps, investigating the model in none periodic forms and/or having applied a kind of noise on the input current can shed more light on the behavior of the DSM neuron model under time varying and also noisy input currents in sense of signal-to-noise ratio and the ability of the model in signal detection.

The results indicate that the neurons are highly capable of making a sophisticated and beneficial use of the channel noise in processing signals. From the engineering point of view, the study reveals the potential appeal of the DSM model for signal detection.

REFERENCES

Bezrukov S. M. and Vodyanoy I., Noise-induced enhancement of signal transduction across voltage-dependent ion channels. Nature 378: 362-364, 1995.

Bezrukov S.M. and Vodyanov, I., Noise-induced enhancements of signal transduction across voltage-dependent ion channels. Nature 378, 362–364, 1995

Braun H.A., Huber M.T., Dewald M., and Voigt K., The neuromodulatory properties of ”Noisy neuronal oscillators”. In: Kadtke J.B. and Bulsara A., Applied nonlinear Dynamics and stochastic systems near the millenium. The American Institute of Physics, 281–286, 1997

Braun H.A., Huber M.T., Dewald M., Sch¨afer, K., and Voigt, K., Computer simulations of neuronal signal transduction: The role of nonlinear dynamics and noise. Int. J. Bif. Chaos 8, 881–889, 1998

Chen Y., Yu L., and Qin S. M., Detection of subthreshold pulses in neurons with channel noise, PHYSICAL REVIEW E 78, 051909, 2008

Chow C. C. and White J. A., Spontaneous action potentials due to channel fluctuations. Biophys. Journal 71: 3013-3021, 1996.

Dayan P. and Abbot L. F., Theoretical Neuroscience Computational and Mathematical Modeling of Neural Systems, MIT Press, 2002

Diba K., Lester H. A., and Koch C., Intrinsic noise in cultured hippocampal neurons: experiment and modeling. J. Neurosci. 24: 9723-9733, 2004.

Faisal A. A., Selen L. P. J., and Wolpert D.M., Noise in the nervous system. Nature Revs. Neurosci. 9:292–303, 2008.

Fox R. F. and Y.N. Lu, Emergent collective behavior in large numbers of globally coupled independently stochastic ion channels. Phys. Rev. E, 49: 3421-3431, 1994.

Gammaitoni L., Hänggi P., Jung P., and Marchesoni F., Stochastic resonance. Rev. Mod. Phys., 70:223-287, 1998.

Gerstner W., Kistler W., Spiking Neuron Models, Single Neurons, Populations, Plasticity, Cambridge University Press, 191, 2002

Gong, P.-L. and Xu, J.-X., Global dynamics and stochastic resonance of the forced FitzHugh-Nagumo neuron model. Phys. Rev. E 63, 031906, 2001

Güler M., Modeling the effects of channel noise in neurons: A study based on dissipative stochastic mechanics. Fluct. Noise Lett. 6:L147-L159, 2006.

Güler M., Dissipative stochastic mechanics for capturing neuronal dynamics under the influence of ion channel noise. Phys. Rev. E, 76, 041918(17), 2007.

Güler M., Detailed numerical investigation of the dissipative stochastic mechanics based neuron model. J. Comput. Neurosci. 25:211–227, 2008.

Haberly L. B., Olfactory cortex, in G. M. Shepherd (ed.), The Synaptic Organization of the Brain, Oxford University Press, New York, chapter 10, pp. 317–345, 1990

Hindmarsh J.L. and Rose R.M., A model of neuronal bursting using three coupled first order differential equations. Proc. R. Soc. Lond. B Biol. Sci. 221, 87–102, 1984

Jacobson G. A. et al., Subthreshold voltage noise of rat neocortical pyramidal neurons. J. Physiology 564: 145-160, 2005.

Jaramillo F. and Wiesenfeld K., Physiological noise level enhances mechanoelectrical transduction in auditory hair cells. Chaos Solitons Fractals 11, 1869–1874, 2000

Jibril G. O. and Güler M., The renormalization of neuronal dynamics can enhance temporal synchronization among synaptically coupled neurons. Proc. Int. Joint Conf. on Neural Networks, 1433-1438, 2009.

Jung P. and Shuai J. W., Optimal sizes of ion channel clusters. Europhys. Lett. 56: 29-35, 2001.

Kitajo K., Nozaki D., Ward, L.M., and Yamamoto, Y., Behavioral stochastic resonance within the human brain. Phys. Rev. Lett. 90, 218103-1, 2003

Kolb B. and Whishaw I. Q., Fundamentals of Human Neuropsychology, Sixth Edition, Worth Publishers, 4: 83, 91, 92, 2009

Kole M. H., Hallermann S., and Stuart G. J., Single Ih channels in pyramidal neuron dendrites: properties, distribution, and impact on action potential output. J. Neurosci., 26: 1677-1687, 2006.

Lee S.-G. and Kim S., Parameter dependence of stochastic resonance in the stochastic Hodgkin-Huxley neuron. Phys. Rev. E 60, 826–830, 1999

Lindner B. and Schimansky-Geier L., Analytical approach to the stochastic FitzHugh-Nagumo system and coherence resonance. Phys. Rev. E 60, 7270-7276, 1999

Lindner B. and Schimansky-Geier L., Coherence and stochastic resonance in a two-state system. Phys. Rev. E 61, 6103–6110, 2000

Longtin A., Bulsara A., and Moss F., Time-interval sequences in bistable systems and the noise-induced transmission of information by sensory neurons. Phys. Rev. Lett. 67, 656–659, 1991

Manjarrez E., Rojas-Piloni G., Mendez I., and Flores, A., Stochastic resonance within the somatosensory system: Effects of noise on evoked field potentials elicited by tactile stimuli. J. Neurosci. 23, 1997–2001. 2003

Nelson E., Derivation of the Schrödinger Equation from Newtonian Mechanics, Phys. Rev. 150, 1079, 1966

Nelson E., Dynamical Theories of Brownian Motion _Princeton University Press, Princeton, NJ, 1967

Nelson M. and Rinzel J., The Hodgkin-Huxley Model in Bower J. M., Beeman D., The Book of Genesis, 4: 34-46, 2003

Rose R. M. and Hindmarsh J. L., Amodel of Thalamic neuron, Proceedings of the Royal Society of London. Series B, Biological Sciences, 1984

Rubinstein J., Threshold fluctuations in N sodium channel model of the node of Ranvier. Biophys. Journal, 68: 779-785, 1995.

Rudolph M. and Destexhe A., Do neocortical neurons display stochastic resonance, J. Comp. Neurosci. 11, 19–42, 2001a

Rudolph, M. and Destexhe, A., Correlation detection and resonance in neural systems with distributed noise sources. Phys. Rev. Lett. 86, 3662–3665, 2001b

Sakmann B. and Neher N., Single-Channel Recording (2nd ed.) New York: Plenum 1995.

Schaefer A.T., Angelo K., Spors H., Margrie T.W., Neuronal Oscillations Enhance Stimulus Discrimination by Ensuring Action Potential Precision, 10.1371/journal.pbio.0040163, 2006

Schmid G., Goychuk I. and Hänggi P. H., Stochastic resonance as a collective property of ion channel assemblies, Europhys. Lett., 56 (1), pp. 22–28, 2001

Schmid G., Goychuk I., and Hänggi P., Stochastic resonance as a collective property of ion channel assemblies. Europhys. Lett. 56: 22-28, 2001.

Schneidman E., Freedman B., and Segev I., Ion channel stochasticity may be critical in determining the reliability and precision of spike timing. Neural Comput. 10: 1679-1703, 1998.

Segev I., Cable and Compartmental Models of Dendritic Trees in Bower J. M., Beeman D., The Book of Genesis, 5: 55, 2003

Steur E., Parameter Estimation in Hindmarsh-Rose Neurons, Traineeship report, 2006

Svirskis G., Kotak V., Sanes D. H., and Rinzel J., Enhancement of Signal-to-Noise Ratio and Phase Locking for Small Inputs by a Low-Threshold Outward Current in Auditory Neurons, The Journal of Neuroscience, 22(24):11019-11025, 2002

Wang Y. and Wang Z. D., Information coding via spontaneous oscillations in neural ensembles. Phys. Rev. E 62, 1063-1068, 2000

Ward L.M., Neimann A., and Moss F., Stochastic resonance in psychophysics and in animal behavior. Biol. Cybern. 87, 91–101, 2002